Mehran University Research Journal of Engineering & Technology
Vol. 37, No. 2, 405-416, April 2018
p-ISSN: 0254-7821, e-ISSN: 2413-7219
DOI: 10.22581/muet1982.1802.16

Numerical Simulation of Mixing of Effluent through Porous Media: The Effects of Local Inertia on the Flow

ZULQARNEN ASADULLAH KHOSO BALOCH[*]†, ABDUL LATIF QURESHI[**], ABDUL RAZAQUE SAHITO[*], AND AHSANULLAH BALOCH[***]

RECEIVED ON 26.04.2017 ACCEPTED ON 13.11.2017

ABSTRACT

The steady–state analytical and numerical solutions are obtained for the mixing of effluent with Newtonian fluid in subsurface. The problem presented in this research work is flow through a channel packed by homogeneous porous media, associated to environmental sciences. Simulations are performed employing a time–marching scheme. Numerical method used in the study is a finite element method, while, the frame of reference is Cartesian coordinate system. Adopted algorithm follow semi-implicit technique through Taylor-Galerkin/Pressure-correction scheme. Analytical solution is Obtained and compared with the numerical predictions. Impact of Darcy's number, influence of change in diffusion coefficient of effluent concentration and time dependent effects of velocity profile is investigated. Numerical predictions are compared against both steady–state and time–dependent analytical solutions obtained in the present study, and observed very good agreement. Various interesting features of the flow are reported. The numerical results exhibit that with increasing fluid inertia, the effluent disperses immediately in flow field when entering from same direction with the flow of fluid. While, increasing dispersion coefficient of effluent at fixed rate of inertia the effluent disperses faster and occupy large area of upstream.

Key Words: Finite Element Method, Numerical Simulation, Newtonian Fluids, PorousMedia, Concentration, Effluent.

1. INTRODUCTION

Mixing of the solute transport in a groundwater ûow is a very exciting and fascinating topic for the researchers. A large amount of theoretical as well as numerical models have been developed, however, only few are referred here [1-6]. Nevertheless, their validity is still under question. Moreover, the importance and its high level of complexity is involved in a large number problem, such as, agricultural, environmental and industrial problems. For instance, seawater incursion in fresh water coastal aquifers and seepage from landûlls have given impetus to the researchers for further investigation of this problem and precise modelling of transport of salt water and develop sophisticated models [7-8].

†Correspondence Author (E-Mail: asadullah.khoso@gmail.com)
* Institute of Environmental Engineering & Management, Mehran University of Engineering & Technology, Jamshoro.
** US-Pakistan Center for Advanced Studies in Water, Mehran University of Engineering & Technology, Jamshoro.
*** Department of Computer Science, ISRA University, Hyderabad.

In the vicinity of coastal areas, the intrusion of sea water in subsurface is a core problem, where fresh groundwater aquifers contaminate. In fact, mixing of saline in freshwater make it inappropriate for human consumption and also reduce the freshwater resources [9]. Therefore, groundwater assets shall be wisely investigated, due to increasing of human population near coastal areas and rising demand in agricultural and industrial use, keeping stability among the saline water and fresh water bodies [10].

A huge percentage of the world's population depend upon groundwater resources and exploits them via private domestic wells or public water supply. Nevertheless, groundwater resources are still now inadequate for human needs in many zones of the world due to various contamination problems. Saline interruption in the subsurface is the most widespread source of contamination to coastal aquifers, however, it is not the only source. Other sources of contamination include leachate from municipal landfills, leaky underground storage tanks that store saline water [11].

For the resolution of density coupled ûow in subsurface, a numerical model has been developed [1], for mass balance equation this model adopts a MHFE (Mixed Hybrid Finite Element) technique. Whilst, for solute transport equation, MHFE is used for dispersion part and DFE (Discontinuous Finite Elements) technique is employed for the convection part respectively. The research work is based on flow of groundwater and solute transport. The model was validated and analysed against two standards test cases of available in the literature [10-13].The authors concluded that MHFE and DFE are more accurate than conforming ûnite elements of [1] and concerning Finite differences of [13].

For inûltration of saline water in homogeneous and saturated subsurface, a 2D (Two-Dimension) numerical model was presented [2], the model was based on mixture of DFE and MHFE methods. Efûciency of numerical solution confirmed on standard benchmarks, for example, the problems of [10-11]. The model was verified against the experimental results obtained by Trinh [14] and the numerical predictions compared with the analytical solutions of Travoix et. al.[15].

2. PROBLEM DEFINITION AND MATHEMATICAL FORMULATION

The problem investigated in this study is effluent mixing, which is mixing of saline water into freshwater; this mixing may be in surface water or may be in subsurface/ groundwater. The schematic diagram of 2D channel is shown in Fig. 1. In reality, near coastal area freshwater aquifers contaminate by seawater intrusion or when flow of freshwater in surface and subsurface, periodically, obstructed by saltwater. However, here, consideration is focused, initially, only on groundwater mixing, i.e. both freshwater and saline water flow in same direction in a channel. Flow is assumed in unidirectional and uniform in a channel, where both side walls are considered solid. While, porous material anticipated isotropic and homogeneous, that reduces the problem into the 1D.

The incompressible two constant viscosity flows of Newtonian fluid past rectangular channel loaded by porous matrix is analysed. CDE (Convection Dispersion Equation) is the most extensively used for the velocity distribution models. The flow is governed by the conservation of mass equation, Darcy's-Brinkman [12] momentum transport equation partially coupled with saline water concentration equation in Cartesian coordinates

frame of reference. In the absence of body force can be presented as:

$$\nabla . u = 0 \tag{1}$$

$$\frac{\rho}{\varepsilon}\frac{\partial u}{\partial t} = \frac{\mu}{\varepsilon}\nabla^2 u - \frac{\rho}{\varepsilon}(u.\nabla)u - \frac{\mu}{k}u - \nabla p \tag{2}$$

$$\frac{\partial S_c}{\partial t} = \eta \nabla^2 S_c - v_{\max}\nabla S_c \tag{3}$$

Where the velocity vector field of fluid is denoted by $\boldsymbol{u}$ = (u,v,w), the absolute viscosity and mass density of the incompressible fluid (per unit liquid volume) is denoted by ρ and μ respectively, and both are supposed to be constant. While, respectively ε and k are the porosity and intrinsic permeability of the porous material, t is the time and the isotropic pressure per unit density denoted by p. Whilst, S_c is the solute concentration of saline water, η is the diffusion–dispersion coefficient of solute concentration and $v_{\max}$ is the maximum water velocity. In Equation (2) the porous medium is assumed homogeneous and isotropic.

In case of unidirectional flow, the components of velocity vector, v and w vanishes. Only velocity component 'u' of axial direction is considered. Therefore, velocity component in axial direction in uniaxial flow condition depend only on transversal 'y' direction $u=f(y)$ and all velocity gradient in 'x' direction become zero. Whereas, the pressure gradient is assumed to be constant in transversal direction 'y' and local convective acceleration disappears also. The Equations (1-3) slashes in 1D as:

$$\frac{\partial u}{\partial x} = 0 \tag{4}$$

$$\frac{\rho}{\varepsilon}\frac{\partial u}{\partial t} = \frac{\mu}{\varepsilon}\frac{\partial^2 u}{\partial y^2} - \frac{\mu}{k}u - \frac{\partial p}{\partial x} \tag{5}$$

$$\frac{\partial S_c}{\partial t} = \eta \frac{\partial^2 u}{\partial y^2} - v_{\max}\frac{\partial S_c}{\partial y} \tag{6}$$

It is often convenient to cast the equations in dimensionless form, adopting non-dimensional unknowns u^*, y^*, t^*, k^*, η^* and S^*_c. To select the suitable choice of characteristics scaling factors, $u = V_c u^*$, $y = L_c y^*$, $k = k^*$ and $t = t^* \rho L_c/\mu$. Where u^* non–dimensional axial velocity component and transversal displacement is represented by y^*. Whereas, k^* is the dimensionless permeability of the porous matrix and t^* is the dimensionless time. Effluent

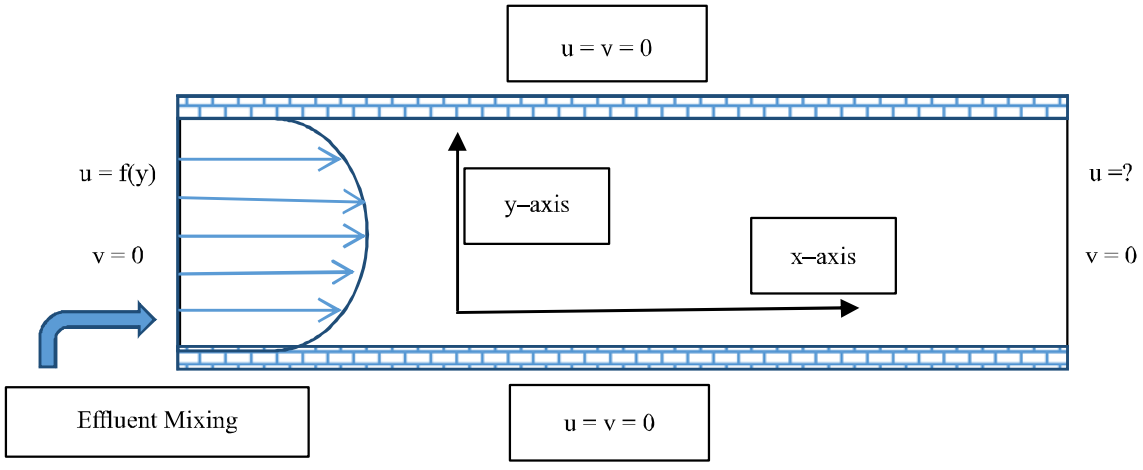

FIG.1. SCHEMATIC DIAGRAM OF TWO–DIMENSIONAL CHANNEL

concentration $S_c = S^*_c S_0$, diffusion–coefficient$\eta = v^* \upsilon \eta$. While, υ is the kinematic viscosity, V_c is the characteristic velocity taken as reference axial velocity $V_c = \frac{\varepsilon L_c^2}{\mu}\left(-\frac{\partial p}{\partial x}\right)$ and L_c is the characteristic length chosen as half width of the channel. In the dimensionless form, the governing system of equations becomes:

$$\frac{\partial u}{\partial x} = 0 \tag{7}$$

$$\frac{\partial u}{\partial t} = 1 + \frac{\partial^2 u}{\partial y^2} - \frac{1}{D_a} u \tag{8}$$

$$\frac{\partial S_c}{\partial t} = D_c \frac{\partial^2 S_c}{\partial y^2} - u_{\max} \frac{\partial S_c}{\partial y} \tag{9}$$

Where dimensionless number and coefficient are as flows:

Darcy's number $\left(D_a = \frac{k^*}{\varepsilon L_c^2}\right)$ and Diffusion–Dispersion coefficient $\left(D_c = \frac{v}{\eta L^2}\right)$

For the flow problem in focus, it is essential to set suitable initial and boundary conditions to provide a well–posed specification. Simulations starts after quiescent initial state $u(0,y) = 0$. Whereas, for velocity component, on both boundary points the conditions are prescribed a as: $u(t,0) = V_{max}$ and $u(t,1) = 0$. While, for concentration equation the initial condition set: $S_c(0,y) = 0$ and for boundary conditions on both points are fixed as: $S_c(t,0) = u_{\max}$ and $S_c(t,1) = 0$.

3. ANALYTICAL SOLUTION

To obtain the analytical solution of the 1D Darcy's-Brinkman momentum Equation (8), conditions follows as:

Initial Condition: $u(0,y) = 0$, whereas, on both boundary points the condition is fixed as: $u(t,0) = u_{\max}$ and $u(t,1) = 0$. The computational domain is $0 < y < 1$.

Here Equation (8) along with it boundary conditions is non–homogeneous, therefore, assuming two function v and H, v is a function of time and space and H is a function of space only as u(t,y) = v(t,y) + H(y).

For conversion into homogeneous partial differential Equation (3) is distributed in two parts as follows:

$$\frac{\partial^2 u}{\partial y^2} = \frac{\partial^2 v}{\partial y^2} + H'' \text{ and } \frac{\partial u}{\partial t} = \frac{\partial v}{\partial t} \tag{10}$$

Then Equation (3) can be written as:

$$\frac{\partial^2 v}{\partial y^2} - \frac{1}{D_a} v + 1 = \frac{\partial v}{\partial t} \tag{11}$$

and

$$H''(y) - \frac{1}{D_a} H(y) = 0 \tag{12}$$

For velocity component 'v', the initial and boundary conditions are changed into homogeneous conditions. The initial condition is set as: v(0,y) = 0 and so on both boundary points condition is fixed as: v(t,0) = 0 and v(t,1) = 0.

3.1 Steady–State Solution

For steady state, the time derivative in Equation (11) vanish $\left(\frac{\partial v}{\partial t} = 0\right)$, hence the Darcy's–Brinkman Equation (11) can be written in ordinary differential equation as:

$$\frac{\partial^2 v}{\partial y^2} - \frac{1}{D_a} v = -1 \tag{13}$$

Equation (13) is simple non–homogeneous ordinary differential equation, subject to homogeneous conditions

on both sides of the domain. For velocity v(t,y), the analytical solution of Equation (13) after some simple mathematical calculation become:

$$\therefore v(y) = Da\left[1 - \frac{\cosh\left(\frac{y-0.5}{\sqrt{Da}}\right)}{\cosh\left(\frac{0.5}{\sqrt{Da}}\right)}\right] \quad (14)$$

Similarly, boundary conditions for H(y) are as: $H(0) = v_{max}$ and $H(1) = 0$, the solution of H(y) become:

$$H(y) = v_{\max}\left[\frac{\sinh\left(\frac{1-y}{\sqrt{Da}}\right)}{\sinh\left(\frac{1}{\sqrt{Da}}\right)}\right] \quad (15)$$

Hence complete solution of steady–state velocity (u) is $u(0, y) = v(0, y) + H(y)$ so that:

$$u(0, y) = Da\left[1 - \frac{\cosh\left(\frac{y-0.5}{\sqrt{Da}}\right)}{\cosh\left(\frac{0.5}{\sqrt{Da}}\right)}\right] - v_{\max}\left[\frac{\sinh\left(\frac{y-1}{\sqrt{Da}}\right)}{\sinh\left(\frac{1}{\sqrt{Da}}\right)}\right] \quad (16)$$

For steady–state solution, graphs are given at different Darcy's numbers through Equation (16). It is observed that, at high Darcy's number ($D_a >> 1$) flow become parabolic, while, at low Darcy's number ($D_a << 1$) the flow behave like plug flow as shown in **Fig. 2(a-b).**

3.2 Unsteady State Solution

The momentum Darcy's-Brinkman Equation (11) is:

$$1 + \frac{\partial^2 v}{\partial y^2} - \frac{1}{D_a} v = \frac{\partial v}{\partial t} \quad (17)$$

While, the condition for initial–state v(0,y) = 0and on the both boundary points condition over the domain of

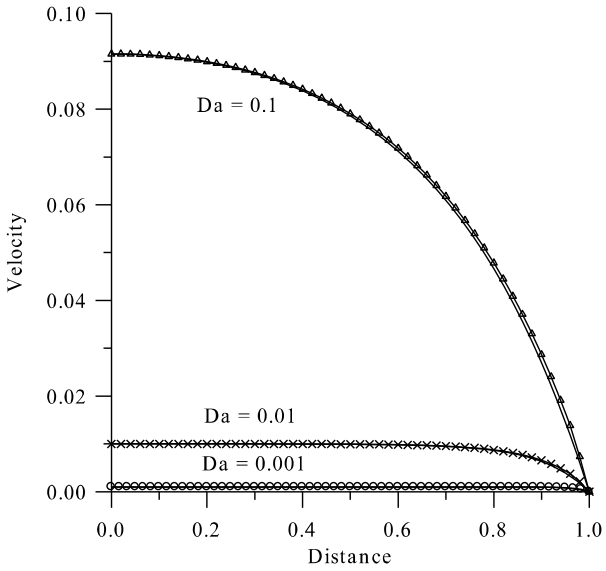

(a) DA = 0.1, 0.01 AND 0.001

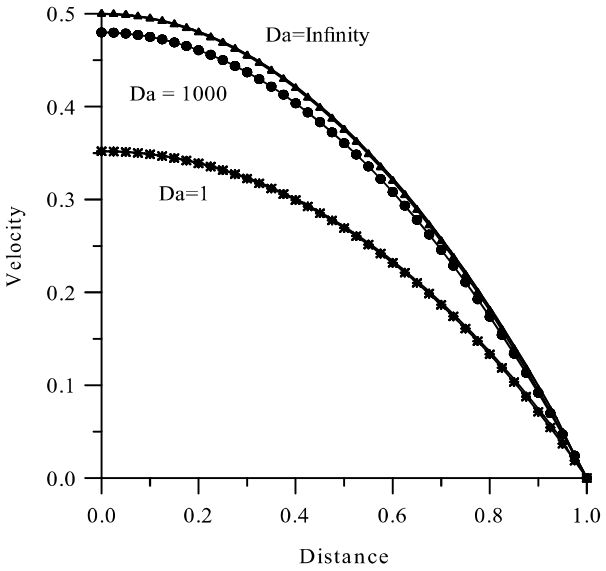

(b) DA = 1, 1000 AND "

FIG. 2. GRAPH OF THE ANALYTICAL AND STEADY–STATE NUMERICAL VELOCITY PROFILE AT DIFFERENT DIMENSIONLESS DARCY'S NUMBER VALUES

interest ($0 < y < 1$) is $v(t,0) = V_{max}$ and $v(t,1) = 0$. Equation (17) is non–homogeneous and boundary conditions at any time are also non–homogeneous.

The Equation (17), subject to the initial and boundary conditions, have been determined through Laplace Transform. For time domain ($t \geq 0$), assuming F(t) be a function then, by definition the integral is:

$L\{F(t)\} = \int_0^\infty e^{-st} F(t)dt = f(s)$, is called Laplace function f(s), in case of integral converges.

As transform of derivative can be defined, if f(t), f'(t),…,f^{n-1}(t), these all functions are continuous over the domain [0,∞]. If f^n(t) is piecewise continuous in the domain of interest [0,∞], then the function is of exponential order.

$$L\{F^n(t)\} = S^n f(s) - S^{n-1} f'(0) - S^{n-2} f''(0) - ..... - f^{n-1}(0)$$

Hence, L{v(t,y)} = V(s,y). So, by applying the Laplace Transform method, we have:

$$L[1] + L\left[\frac{\partial^2 v}{\partial y^2}\right] - \frac{1}{Da} L[v] = L\left[\frac{\partial v}{\partial t}\right] \quad (18)$$

This implies that:

$\frac{d^n V(s,y)}{dy^2} - \left(\frac{1}{Da} + s\right) V(s,y) + \frac{1}{s} = 0$, subject to homogeneous boundary conditions. V(s,-1) = V(s,1) = 0. Then the result of Equations (18-19) is given as:

$$V(s,y) = \frac{1}{s\left(s + \frac{1}{Da}\right)} - \frac{Cosh\sqrt{\frac{1}{Da} + s}}{s\left(s + \frac{1}{Da}\right) Cosh\sqrt{\frac{1}{Da} + s}} \quad (19)$$

Apply Inverse Laplace transform of equation can be solved by residues theorem and the result is given as:

$$v(t,y) = Da\left(1 - \frac{Cosh\sqrt{\frac{1}{Da}}y}{Cosh\sqrt{\frac{1}{Da}}}\right) - \sum_{n=0}^{\infty} \frac{2(-1)^n e^{-\left(\beta_n^2 + \frac{1}{Da}\right)t} Cos\beta_n y}{\left(\beta_n^2 + \frac{1}{Da}\right)\beta_n} \quad (20)$$

Where $\beta_n = (2n-1)\frac{\pi}{2}$

The analytical solutions Equation (20) of Equation (17) achieved by using Laplace Transform techniques at different values of time t with unit value of Darcy's number.

For the time dependent solute concentration Equation (9) an analytical solution is obtained after some simple mathematical calculation adopting similar approach and also has been given by Ogata and Banks [16] as:

$$S_c(y,t) = \frac{S_c}{2}\left[erfc\left(\frac{y-ut}{2\sqrt{D_c t}}\right) + \exp\left(\frac{uy}{\sqrt{D_c}}\right) erfc\left(\frac{y+ut}{2\sqrt{D_c t}}\right)\right] \quad (21)$$

Where erfc is the complementary error function. Erfc(v) =1 – erf(v), where, erf is the error function, $erf(v) = \frac{2}{\pi}\int_0^v e^{-u^2} du$

4. NUMERICAL SCHEME

In this study a time-marching finite element numerical scheme adopted for the simulations. For time derivative, this scheme use Taylor series expansion in multi–stages to discretise temporal domain. At half time step, forward difference is applied to achieve the solution from initial state, while for full time step, central difference is employed using both initial state information and solution of half time step. While, for spatial discretisation, Galerkin approach is adopted. For pressure gradient and viscous diffusion terms a Crank–Nicolson approach is used. In this way a semi–implicit scheme is achieved here. This scheme was tested and

proved efficient by Qureshi and Baloch [17]. Through this approach a second and higher order accuracy is attended. Furthermore, the details are given in the previous studiesof Mahessar et. al. [18] and Shaikh [19].

For both, velocity and concentration, quadratic finite elements approximations are adopted. To obtained accurate and close to analytical solution eighteen numbers of elements for single momentum equation, whilst, for both equations thirty-six elements appears to be more appropriate choice to adopt**.** For time marching, stabilise the solution process tolerance for Δt is taken $\varepsilon = 10^{-5}$ and to terminate the procedure, a relative least square increment $\sqrt{\frac{\sum_{i=1}^{N}\left|u_i^{n+1}-u_i^{n}\right|^2}{\sum_{i=1}^{N}\left(u_i^{n+1}\right)^2}}$ is chosen.

Finite Element semi–implicit form of fully discrete system in compact matrix formulation

From dimensionless Equations (8-9), the fully-discretised formulation is:

Step-1: Compute velocity component and concentration of effluent at half time step (n+1/2) from given information at initial level (*n*):

$$\left(\frac{2M}{\Delta t}+\frac{S}{2}\right)\left(U_j^{n+\frac{1}{2}}-U_j^{n}\right)=M_p-\left[S+\frac{1}{D_a}M\right]U_j^{n} \qquad (22)$$

$$\left(\frac{2M}{\Delta t}+\frac{D_cS}{2}\right)\left(C_j^{n+\frac{1}{2}}-C_j^{n}\right)=\left[D_cS-N\left(U^{n}\right)\right]C_j^{n} \qquad (23)$$

Step-2: Compute velocity component and concentration of effluent at full time step (n + 1) from given information at initial (*n*) and half time step (n+1/2) levels:

$$\left(\frac{M}{\Delta t}+\frac{S}{2}\right)\left(U_j^{n+1}-U_j^{n}\right)=M_p-\left[SU_j^{n}+\frac{1}{D_a}MU_j^{n+\frac{1}{2}}\right] \qquad (24)$$

$$\left(\frac{2M}{\Delta t}+\frac{D_cS}{2}\right)\left(C_j^{n}-C_j^{n}\right)=\left[D_cSC_j^{n}-N\left(U^{n+\frac{1}{2}}\right)C_j^{n+\frac{1}{2}}\right] \qquad (25)$$

Where pyramids are defining in (Shaikh, [16]).

5. NUMERICAL RESULTS AND DISCUSSION

5.1 Impact of Darcy's Number

At different low values of D_a (0.001, 0.01 and 0.1) and D_a (=10) near wall effluent slowly diffused whilst, velocity behaviour shows plug flow at D_a (=0.01 and lower) with increasing D_a (=0.01 and 0.1) shows a parabolic. Similarly, with increasing D_a (1.0, 1000, and ∞), the behaviour of effluent and velocity is same as lower Darcy's, as illustrated in Fig. 3(a-b).

Different low values of Darcy's (=0.001, 0.01 and 0.1) are used and with increasing D_c (=1000) near wall effluent is immediately diffused whilst, velocity behaviour shows plug flow at lowest Da and with increasing D_a the velocity behaviour shows a parabolic as displayed in Fig. 4(a-b). Similarly, at higher Darcy's (=1 to Infinity) and with increasing D_c (= 1000) near wall effluent is sharply diffused. Whilst, velocity behaviour shows a parabolic. With increasing D_c (= 5000), the effluent is too sharply diffused at lower and higher Darcy's as exhibited in Fig. 5(a-b).

5.3 Time Dependent Effects of Velocity Profile at Lower and Higher Darcy Numbers.

At low values of Darcy's number, the flow behaviour of velocity profile shows plug flow at D_a (= 0.001 and 0.01) with sharp boundary layer likewise plug flow, whilst, at D_a (=0.1) with thick boundary layer at same corresponding order of maximum value as presented in Fig. 6(a-b). At higher values of Darcy's, the development of time dependent velocity profile increase and behaviour of velocity shows finally parabolic.

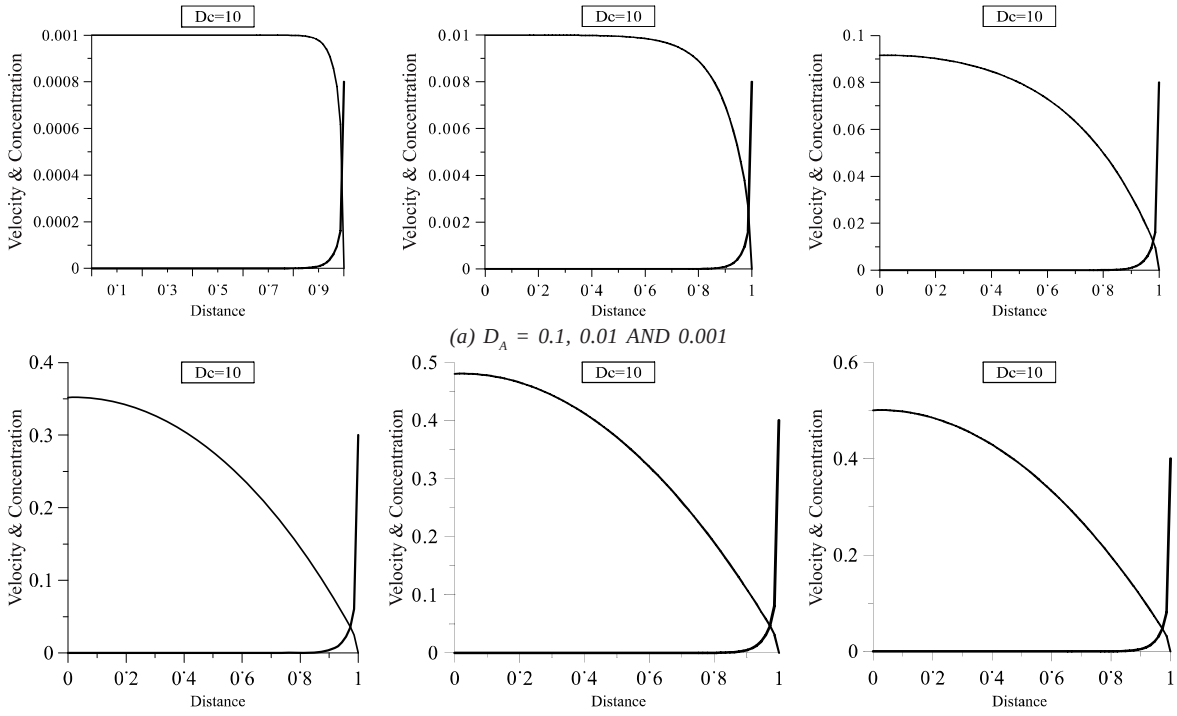

(a) D_A = 0.1, 0.01 AND 0.001

(b) D_C = 10

FIG. 3. STEADY–STATE NUMERICAL SOLUTION AT FIXED DIFFUSION COEFFICENT OF CONCENTRATION AND DIFFERENT DIMENSIONLESS DARCY'S NUMBER VALUES

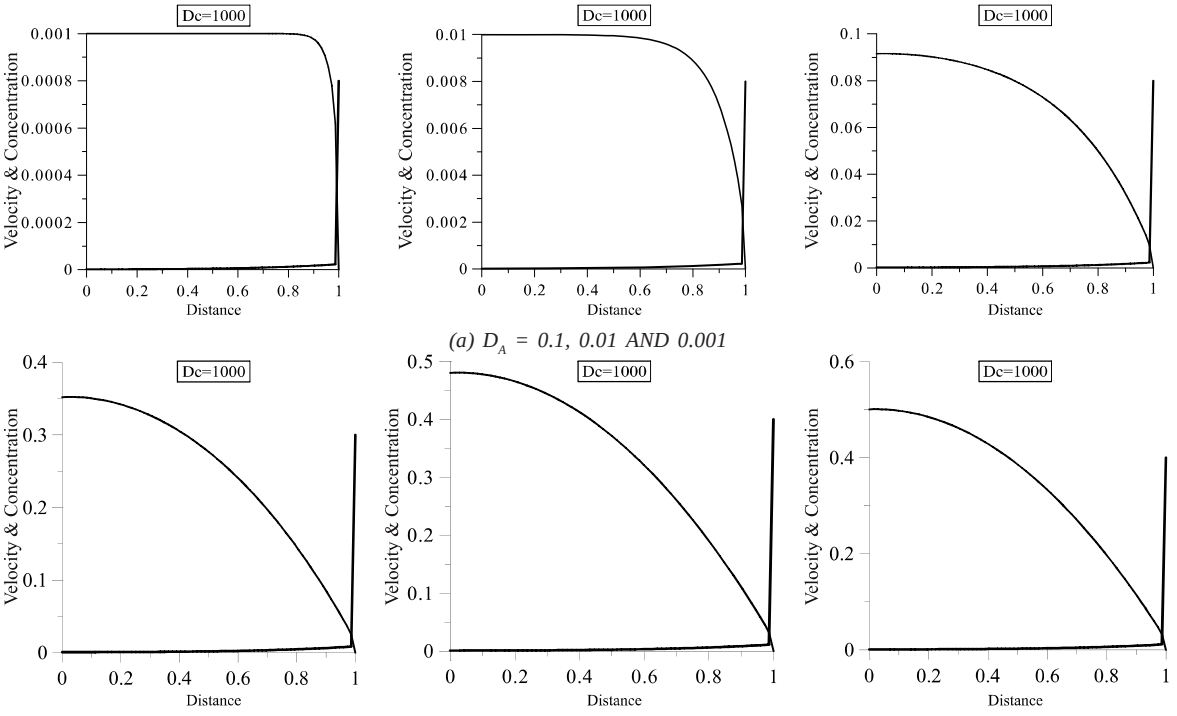

(a) D_A = 0.1, 0.01 AND 0.001

(b) FIXED D_C = 1000 VALUE

FIG. 4. STEADY–STATE NUMERICAL SOLUTION AT DIFFERENT DARCY'S VALUES

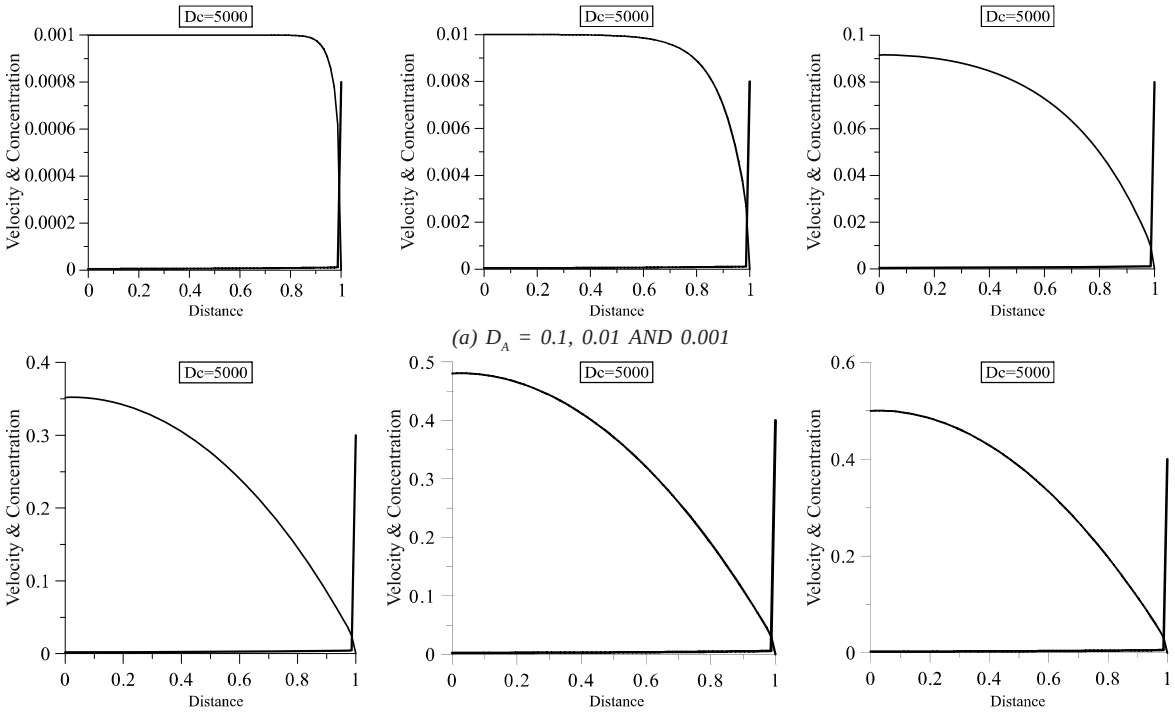

(a) D_A = 0.1, 0.01 AND 0.001

(b) FIXED D_C = 5000 VALUE

FIG. 5. STEADY–STATE NUMERICAL SOLUTION AT DIFFERENT DIMENSIONLESS DARCY'S NUMBER VALUES

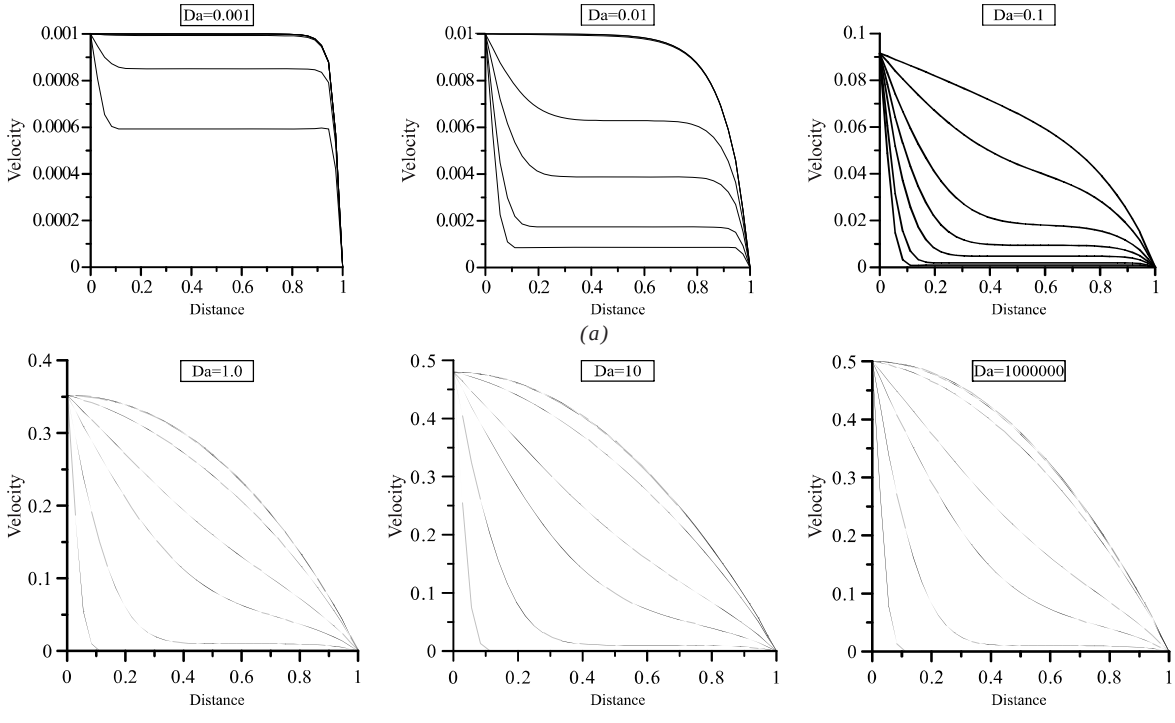

(a)

(b)

FIG. 6. TIME–DEPENDENT NUMERICAL SOLUTION AT INCREASING DIMENSIONLESS DARCY'S NUMBER VALUES FROM D_a = 0.1 TO 100000 AND VARYING TIME STARTING FROM INITIAL–STATE TO STEADY–STATE

6. CONCLUSION

For the mixing of effluent with unidirectional flow of Newtonian fluid in the presence of porous material, the steady–state numerical prediction as well as analytical solutions are realised. For numerical prediction a time–marching finite element scheme is used. From the 1D results, two step semi–implicit Taylor–Galerkin, algorithm is adopted. A very good agreement is achieved between analytical and numerical predictions.

The impact of Darcy's number, influence of change in diffusion coefficient of effluent concentration and time dependent effects are displayed in different figures and field plots are analysed. Also, the validities of results are shown through velocity and concentration profiles, reported through graphs. It is concluded that the velocity profile, initially, with fixed concentration (Dc) demonstrates a plug flow at small values of Darcy's number, while increasing Darcy's number flow profile become parabolic. Whilst, at inlet the concentration profile of effluent exhibits very slow growth, whereas, at exit develop rapidly. While, time–dependent effects displayed, initially, gentle progress in velocity profile is observed and the similar phenomena at steady–state case as well perceived.

7. NOMENCLATURE

x	Axial Coordinate
y	Transverse Coordinate
V	Axial velocity
p	Pressure
D_a	Darcy's number
t	Time
V_c	Reference Axial Velocity
x^*	Dimensionless Axial Coordinate, x/L
y^*	Dimensionless Transverse Coordinate, y/L
V^*	Dimensionless Axial velocity, $u=u_0$
L	Half Channel width
D_c	Dispersion Coefficient
t^*	Dimensionless Time

Greek Symbol

ε	Porosity of the Porous Media
ρ	Fluid Density
k	Intrinsic Permeability of the Porous Medium
μ	Dynamic Viscosity
k^*	Modified Permeability of the Porous Medium

ACKNOWLEDGEMENTS

The first author is grateful to Prof. Dr. Rasool Bux Mahar, US-Pakistan Centre for Advanced Studies in Water, for his helpful guidance and comments. Authors also acknowledges the Institute of Environment Engineering & Management, Mehran University of Engineering & Technology, Jamshoro, Pakistan.

REFERENCES

[1] Ackerer, Ph., Younes, A., and Mose, R., "Modelling Variable Density Flow and Solute Transport in Porous Medium: 1. Numerical Model and Veriûcation", Transport in Porous Media, Volume 35, No. 3, pp. 345-373, 1999.

[2] Oltean, C., and Bues, M.A., "Inûltration of Salt Solute in Homogeneous and Saturated Porous Media–An Analytical Solution Evaluated by Numerical Simulations", Transport in Porous Media, Volume 48, No. 1, pp. 61-78, 2002.

[3] Guerrero, J.S.P., Skaggs, T.H., and Van Genuchten, M.T., "Analytical Solution for Multi-Species Contaminant Transport in Finite Media with Time-Varying Boundary Conditions", Transport Porous Media, Springer, 2010.

[4] Selvadurai, A.P.S., and Dong, W., "Modelling of Advection-Dominated Transport in a Porous Column with a Time-Decaying Flow Field", Transport in Porous Media, Volume 63, No. 2, pp. 261-288, 2006.

[5] Zhang, Q., Volker, R.E., and Lockington, D.A., "Numerical Investigation of Seawater Intrusion at Gooburrum, Bundaberg, Queensland, Australia.", Hydrogeology Journal, Volume 12, No. 6, pp. 674-687, 2004.

[6] Voss, C.I., Simmons, C.T., and Robinson, N.I., "Three-Dimensional Benchmark for Variable-Density Flow and Transport Simulation: Matching Semi-Analytic Stability Modes for Steady Unstable Convection in an Inclined Porous Box", Hydrology Journal, Volume 18, pp. 5-23, 2010.

[7] Sherif, M.M., and Singh, V.P., "Effect of Groundwater Pumping on Seawater Intrusion in Coastal Aquifers", Journal of Agricultural and Marine Sciences, Volume 7, No. 2, pp. 61-67,2002.

[8] Hogan, M.B., "Understanding the Flow and Mixing Dynamics of Saline Water Discharged Into Coastal Freshwater Aquifers", M.Sc. Thesis, Graduate Faculty of Auburn University, Auburn, 2006.

[9] Hanf, L.F.M., Poston, T.M., and Dirke, R.L., "Summary of the Hanford Site: Environmental Report for Calendar Year 2004", Richland, WA, Pacific Northwest Laboratory/USDepartment of Energy, 2005.

[10] Henry, H.R., "Interfaces between Saltwater and Freshwater in Coastal Aquifers", US Geological Survey Water-Supply Paper 1613-C, Sea Water in Coastal Aquifers: C35–C70, 1964.

[11] Elder, J.W., "Transient Convection in a Porous Medium", Journal of Fluid Mechanics, Volume 27, pp. 609-623, 1967.

[12] Kaaschieter, E.F., "Mixed Hybrid Finite Elements for Saturated Groundwater Flow", Gambolati, G., Rinaldo, A., Brebbia, C.A., Gray, W.G., and Pinder, G.F., (Editors), Computational Methods in Subsurface Hydrology, Computational Mechanics, Southampton, pp. 17-22, 1990.

[13] Mos´e, R., Siegel, P., Ackerer, P., and Chavent, G., "Application of the Mixed Hybrid Finite Element Approximation in a Groundwater Flow Model: Luxury or Necessity?", Water Resource Research, Volume 30, No. 11, pp. 3001-3012, 1994.

[14] Trinh, T.B., "Inûltration Par Contraste de Densit´ e en Entrainement d'un Liquide Miscible Emis ` ad´ ebit Constant dans un Milieu Poreux Satur´ e d'eau au Repos ou en Mouvement", Ph.D. Thesis, Universit´ e Louis Pasteur, Strasbourg, pp. 109, France, 1974.

[15] Triboix, A., Trinh T.B., and Zilliox, L., 'Th´ eorie de la Dispersion sous l'effet d'un Contraste de Densit´ e: Inûltration d'un Liquide Miscible dans un Milieu Poreux Satur´ e d'eau en Repos", CR Academic Science, 280, pp. 1713-1716, Paris,1975.

[16] Ogata, A., and Banks, R.B., "A Solution of the Differential Equation of Longitudinal Dispersion in Porous Media", US Geological Survey, Paper 411–A, 1961.

[17] Qureshi, A.L., and Baloch, A., "Finite Element Simulation of Sediment Transport: Development, Validation and Application of Model to Potho Minor of Jamrao West Branch, Sindh, Pakistan", Article No. 230, Advances in River Sediment Research, Fukuoka, et. al. (Editor), CRC Press Book, Taylor and Francis Group, London, UK, September, 2013.

[18] Mahessar, A.A., Baloch, A., and Qureshi, A.L., "Solution of Diffusion Wave Equation Using FEM for Flood Routing", Mehran University Research Journal of Engineering & Technology, Volume 33, No. 3. pp. 209-214, Jamshoro Pakistan, July, 2014.

[19] Shaikh, H., "Numerical Simulation of Expansion and Contraction Flow in Channel Filled with Porous Media", Ph.D. Thesis, Department of Mathematics, Shah Abdul Latif University, Khairpur Mirs, Pakistan, 2016.